

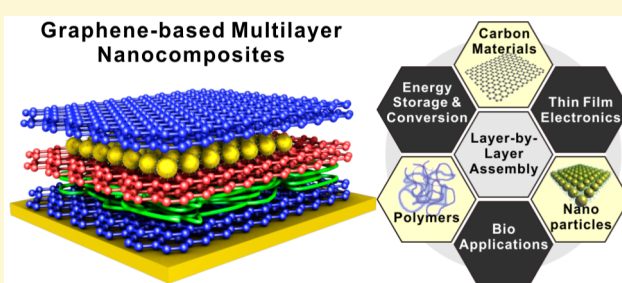
Layer-by-Layer Assembly for Graphene-Based Multilayer Nanocomposites: Synthesis and Applications

Taemin Lee,^{||,†} Sa Hoon Min,^{||,†} Minsu Gu,^{||,†} Yun Kyung Jung,^{||,†} Wonoh Lee,[‡] Jea Uk Lee,[‡] Dong Gi Seong,[‡] and Byeong-Su Kim^{*,†,§}

[†]Department of Energy Engineering and [§]Department of Chemistry, Ulsan National Institute of Science and Technology (UNIST), Ulsan 689-798, Korea

[‡]Composites Research Center, Korea Institute of Materials Science (KIMS), 797 Changwon-daero, Changwon, Gyeongnam 642-831, Korea

ABSTRACT: Two-dimensional (2D) graphene sheets have become a versatile platform for the fabrication of innovative hybrid materials with various functions due to their unique electrical, optical, thermal, and mechanical properties. The preparation of graphene-based composites with nanoscale precision is highly important for reproducible and controllable performance through the analysis of interplay between each component. In particular, the layer-by-layer (LbL) assembly technique is known as a simple, inexpensive, and versatile process for the fabrication of highly ordered multilayer film structures from various types of materials. The LbL structures capable of controlling nanoscale composition and architectures are achieved through the sequential adsorption of oppositely charged components by attractive forces such as electrostatic interactions. In this review, we will focus on the recent progress in graphene-based nanocomposites hybridized with various nanomaterials such as carbon nanomaterials, polymers, and inorganic nanoparticles by the LbL assembly. Multilayered graphene nanocomposites exhibit improved physical/chemical properties and superior performance compared with the individual components due to the synergistic effects in various applications including electric devices, energy storage and conversion, and biological usages.



1. INTRODUCTION

There have been active investigations to produce novel materials with unique physical/chemical properties by hybridizing more than two different nanomaterials. These high-performance hybrid materials have been widely employed in various applications ranging from electrical devices (transparent conducting films (TCFs), field effect transistors) and energy storage and generation (batteries, supercapacitors, and solar cells) to biological usages (biosensing, bioimaging, and drug delivery). However, the preparation of homogeneous hybrid materials based on two-dimensional (2D) nanosheets such as graphene is rather challenging due to strong van der Waals attraction between the materials.

Graphene, which is composed of a one-atom-thick sp^2 -carbon lattice, has drawn tremendous interest in the materials science and engineering field because of its extraordinary electrical, optical, thermal, and mechanical properties.^{1–3} Chemically exfoliated graphene oxide (GO) sheets are well dispersed in aqueous solution due to their charged functional groups such as carboxylic acids and alcohol groups.^{4,5} Moreover, their chemical stability and high conductivity in addition to their high surface area allows these 2D sheets to act as excellent substrates for hosting and growing functional nanomaterials, including other carbon allotropes, inorganic nanostructures, polyelectrolytes, and biomolecules. Although

the intrinsic structural defects often lead to a deterioration of the material properties and performance compared with pristine graphene, GO can offer a versatile platform for innovative hybrid materials with unique properties.

Several studies have reported that graphene-based hybrid composites exhibit superior performance compared with the individual components because of the synergistic effects between each component. As a representative example, the addition of graphene into hybrid composites provides 2D conducting channels for charge transfer during the electrochemical reactions.^{6–8} Simultaneously, graphene employed as a large surface area support, which was easily exposed to the electrolyte and oxygen as well as effectively accelerating reactant, ion, and electron transport. Thus, the formation of graphene-based composites is greatly advantageous to the design of a new type of versatile material for high-performance TCFs, field-effect transistors (FETs), sensors, supercapacitors, solar cells, lithium ion batteries, electrodes, drug carriers, gas barriers, photocatalysts, and photoconductors. In many cases, however, graphene-based composites are highly disordered, leading to difficulties in demonstrating their reproducible

Received: February 8, 2015

Revised: May 3, 2015

Published: May 4, 2015

performance and analyzing the contribution of each material to the device characteristics. One possible route to achieve nanoscale uniformity of these composites while preserving the unique characteristics of their constituents is to use layer-by-layer (LbL) assembly. The LbL technique is achieved through the sequential adsorption of oppositely charged components by attractive forces such as electrostatic interactions, hydrogen bonding, etc. Thus, the highly ordered and multilayered architectures by LbL assembly can be manufactured reproducibly, allowing nanoscale-level control of the thickness and composition of hybrid composite materials.

Although there are excellent reviews in the area of nanocomposites based on the LbL approach,^{9–15} recent studies on graphene as an active component of LbL assembly are still limited. In this review, we will outline the recent progress in this field with a particular focus on the contribution of our studies. Moreover, the review is presented with the counterpart of the graphene nanocomposites that are complexed, such as other carbon nanomaterials, polymers, and inorganic nanomaterials, in various device applications, including flexible electrodes, supercapacitor, batteries, and sensors (Figure 1).

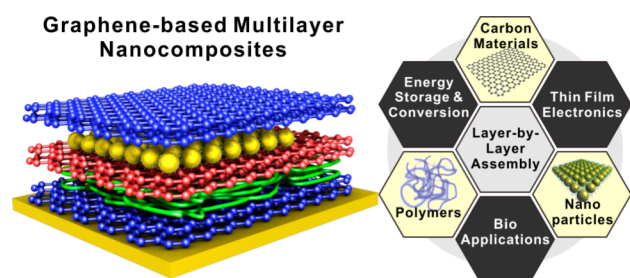


Figure 1. Summary of the applications of graphene-based nanocomposites prepared by layer-by-layer (LbL) assembly.

2. LAYER-BY-LAYER (LbL) ASSEMBLY

The initial idea of LbL assembly was first presented by Iler in 1966, who demonstrated the deposition of oppositely charged silica and alumina particles.¹⁶ Decher and co-workers revived

LbL assembly by making thin films via the alternate adsorption of oppositely charged polyelectrolytes.¹⁷ Until recently, LbL approaches have attracted substantial attention due to the versatility of readily tailoring the size, composition, porosity, stability, and surface functionality of the resulting thin films by incorporating multiple functionalities using a facile and inexpensive process.

LbL-assembled thin films are prepared via the sequential adsorption of different macromolecular components exhibiting attractive forces such as electrostatic interactions, hydrogen bonding, van der Waals forces, and charge transfer complexes.¹¹ Graphene-based LbL assembly was first demonstrated by using non-exfoliated graphite oxide platelets and polyelectrolyte by Kotov et al. in 1996.¹⁸ Three years later, a well-exfoliated individual graphite oxide sheet was used with cationic polymer for LbL growth by Mallouk and Kovtyukhova.¹⁹ A remarkable achievement on the physical properties of graphene sheets by Geim, Novoselov, and others³ renewed significant interests in graphene-based layered materials. The essentials of our review is to show that the introduction of functional groups into graphene during the exfoliation process together with additional chemical modification enables graphene derivatives to be incorporated within LbL-assembled structure by electrostatic interactions, hydrogen bonding, and van der Waals interactions even without the aid of other heterogeneous materials, which is not possible in pristine graphene. Especially, we focus on graphene-based LbL films prepared by the electrostatic attractions between negatively charged GO and positively charged materials (carbon nanomaterials, polymers, and inorganic nanomaterials). These thin film composites prepared by the hierarchical organization would be beneficial for reliable applications over other conventional methods such as vacuum-assisted filtration and Langmuir–Blodgett method. Vacuum-assisted filtration is advantageous to rapid and scale-up fabrication of layered films and has no limitation for selection of materials because the films can be manufactured through the physical trapping of materials using vacuum force.^{11,20} Langmuir–Blodgett film deposition is also preferable for achieving uniform and dense packing of monolayers.^{21,22} However, since the LbL assembly guarantees a nanoscale uniformity of composites and does not require relatively

Table 1. Summary of Graphene/Carbon Hybrids Based on LbL Assembly

material combination		substrate	system (n = no. of layers)	applications	ref
(+) component	(-) component				
MWCNT ^a	MWCNT	ITO/glass	(MWCNT/MWCNT) _n	TCF	27
MWCNT	MWCNT	PDMS	(MWCNT/MWCNT) _n	TCF	28
MWCNT	MWCNT	ITO/glass	(MWCNT/MWCNT) _n	TCF	29
MWCNT	GO	ITO/glass	PDDA/(rGO/MWCNT) _n	biosensor	30
MWCNT	rGO ^b	ITO/PET	(MWCNT/rGO) _n	TCF	4
GO	GO	Si wafer	(GO/GO) _n	FET	23
GO	GO	Si wafer	(GO/GO) _n	FET	31
GO	GO	glass	(GO/GO) _n	biosensor	32
GO	GO	glass	(GO/GO) _n	/	33
rGO	rGO	quartz	(rGO/rGO) _n	TCF	34
rGO	rGO	quartz	(rGO/rGO) _n	TCF	5
APTMS ^c	GO	glass	(APTMS/GO) _n	FET	35
GNR ^d	GNR	Si wafer	(GNR/GNR) _n	FET	36
GO	GO	yeast	(GO/GO) _n	biocapsule	37
rGO	rGO	polystyrene	(rGO/rGO) _n	graphene ball	38

^aMultiwalled carbon nanotubes. ^bReduced graphene oxide. ^c(3-Aminopropyl)trimethoxysilane. ^dGraphene nanoribbons.

specialized skills and instrumentation, it is the most appropriate method to tunable hybrid architecture with a nanoscale precision.

With the progress of LbL assembly, many efficient and commercially feasible deposition methods have been developed. Beyond the most popular and traditional dipping method, spin- and spray-assisted LbL assemblies have been introduced as alternative methods.^{23–26} These new assembly methods often result in well-defined multilayer films as well as a highly ordered internal structure within a very short deposition period. In both methods, besides the electrostatic interactions, various forces such as centrifugal forces, air-shear forces, and flow rate could affect the quality of the resulting LbL films. In particular, spray-assisted LbL deposition is a powerful tool for preparing multilayer films not only on 2D but also on 3D substrates such as complex textile fabrics. The advancement in these different deposition methods has significantly accelerated the applications of LbL assembly to various fields.

3. GRAPHENE/CARBON ASSEMBLY

The hybridization of the unique electrical/chemical properties of carbon nanomaterials with the exceptional versatility of the nanoscale construction of multilayer LbL films has opened up wide research opportunities. In addition, various functionalities can be achieved by the carbon nanomaterials through a facile chemical modification, which makes it easy to host and grow the functional nanomaterials on the surface of carbon nanomaterials. Thus, this approach offers virtually unlimited opportunities for expanding the material selection for LbL deposition.^{28,30,35,36} We summarize the various graphene/carbon multilayered films prepared by LbL assembly and their wide range of applications in Table 1.

3.1. Carbon Nanotubes. Carbon nanotubes (CNTs), one-dimensional (1D) tubular carbon nanomaterials, have been extensively researched in material communities over the past decades because these materials exhibit superior electrical conductivity and high flexibility with large aspect ratios (typically >1000) that makes them ideal reinforcing agents in hybrid materials. However, pristine carbon nanomaterials do not possess intrinsic surface charges and lack colloidal stability in aqueous media; thus, additional treatment steps are required to make these materials useful for LbL engineering.

Hammond and co-workers first reported LbL film of multiwalled carbon nanotubes (MWCNTs) exclusively, where the electrostatic interaction between MWCNTs was induced by charge-selective surface modification (Figure 2a).^{27,29} Negatively charged MWCNTs (MWCNT-COO⁻) were prepared by functionalization with carboxylic acid groups via typical chemical oxidation method, and further surface modification with ethylenediamine in the presence of thionyl chloride, SOCl₂, yielded positively charged MWCNTs (MWCNT-NH₃⁺). The all-MWCNT thin films were simply fabricated by dipping into respective surface functionalized MWCNT solutions and exhibited high electronic conductivity with improved ion transport networks for electrochemical energy applications. Furthermore, they prepared different morphologies of MWCNT multilayers by varying the assembly pH condition and heat treatment, which strongly affect the surface topology and inner structure of MWCNT thin films and eventually resulted in precisely controlled electrochemical properties of the LbL-assembled MWCNT electrode.

Due to the structural similarity of graphene and CNTs, we reported a simple, novel strategy for creating multilayered thin

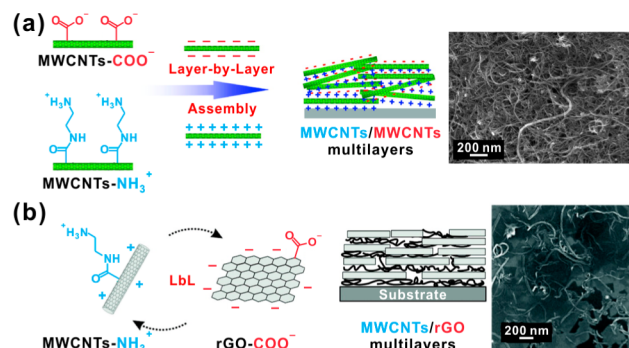


Figure 2. (a) LbL assembled MWCNT thin film with positively and negatively charged MWCNTs. Reprinted with permission from ref 27. Copyright 2008 American Chemical Society. (b) Hybrid LbL multilayers of MWCNTs and rGO. Reprinted with permission from ref 4. Copyright 2010 American Chemical Society.

films of highly conducting reduced graphene oxide (rGO) sheets with MWCNTs via LbL assembly (Figure 2b).⁴ We constructed hybrid multilayers employing the electrostatic interactions between positively charged MWCNTs and negatively charged exfoliated rGO sheets. The integration of MWCNTs not only provides the electronic conductivity but also affords mechanical flexibility of the hybrid film, allowing the electronic contact of graphene sheets by bridging the gaps between graphene sheets. The assembled MWCNTs/rGO hybrids possess high electrical conductivity and transparency with a sheet resistance of 8 kΩ/sq and a transparency of 81% at 550 nm while allowing significant flexibility.

Thus, the utilization of both advantages of the intrinsic properties of functionalized carbon nanomaterials and precise control of the LbL system offers a unique potential platform for advanced electronic, energy, and sensor applications.

3.2. Graphene. **3.2.1. LbL-Assembled Graphene Multilayers.** As a new emerging nanomaterial for thin film electronics, 2D graphene sheets derived from bulk graphite have been significantly considered as the thinnest functional nanomaterial because of an atomic scale thickness and infinite planar dimensions with unique physicochemical properties. In particular, assembly of graphene sheets into macroscopic structures possesses excellent mechanical performance, optical transparency, and good electrical conductivity, due to the contribution of intrinsic properties of individual graphene sheets and the highly ordered architecture of multilayered graphene films. These 2D graphene multilayers can be constructed through the conventional multiple transfers of CVD-grown graphene,^{39–42} vacuum-assisted filtration,^{43,44} and Langmuir–Blodgett method.⁴⁵ However, these approaches suffer from a lack of uniformity, difficulty in precisely controlling the film size and thickness, and low production efficiency.

As a promising approach for the fabrication of graphene multilayers, LbL assembly can create highly tunable, conformal thin films and functional surfaces with nanometer-scale control over the film composition and structure. More specifically, the physicochemical characteristics of multilayered thin films can be tunable by controlling many parameters such as pH, ionic strength, and solute concentration of the solution, which have an impact on thickness, composition ratio, and porosity of the assembled films.

Recently, several studies have reported an integration of the GO sheets into the multilayers by LbL assembly process, which

can create highly controllable thin films in terms of thickness, transmittance, and sheet resistance.^{5,33,34} To introduce the GO into an LbL system based on the electrostatic interactions, we prepared stable GO suspensions through the modified Hummers method that are highly stable and negatively charged over a wide range of pH conditions (GO-COO^-). Positively charged GO sheets (GO-NH_3^+) were subsequently prepared by introducing amine groups ($-\text{NH}_2$) on the surface of negatively charged GO sheets through the *N*-ethyl-*N'*-(3-dimethyl aminopropyl)carbodiimide methiodide (EDC)-mediated reaction between the carboxylic acids and excess ethylenediamine (Figure 3). The sheet resistance and trans-

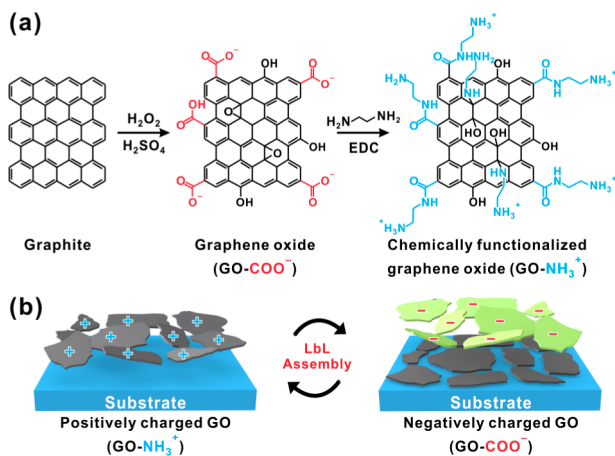


Figure 3. (a) Schematic representation of chemical functionalization with amine groups ($-\text{NH}_2$) on the surface of negatively charged GO sheets through the *N*-ethyl-*N'*-(3-dimethyl aminopropyl)carbodiimide methiodide (EDC)-mediated reaction. (b) The generation of graphene thin films using an electrostatic LbL assembly between oppositely charged graphene sheets.

mittance of LbL-assembled graphene films can be easily tunable in conjunction with the number of bilayers which is strongly related to the thickness of the multilayers by taking advantage of nanoscale engineering of the LbL assembly.

A highly tunable LbL-assembled GO film can be devised for high-throughput multiplex protein sensing (Figure 4a).³² The fluorescence of different target-bound aptamers labeled with dye is efficiently quenched by the GO film through fluorescence resonance energy transfer (FRET), and simultaneous multiplex target detection is performed by recovering the quenched

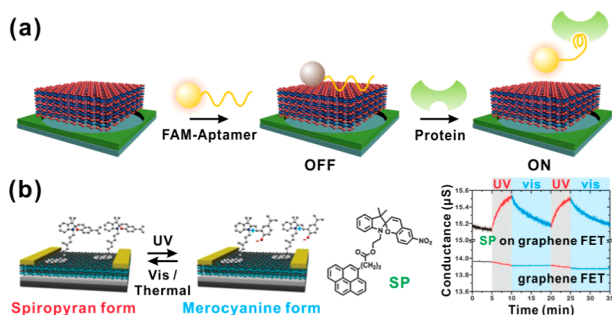


Figure 4. Graphene multilayers for (a) biosensor and (b) photo responsive optoelectronic device. Reprinted with permission from ref 32. Copyright 2013 Nature Publishing Group. Reprinted with permission from ref 31. Copyright 2012 Royal Society of Chemistry.

fluorescence caused by specific binding between an aptamer and a protein. The LbL GO films consisting of 10 bilayers displayed a high quenching ability, yielding over 85% fluorescence quenching with the addition of 2 mM dye-labeled aptamer. The limit for human thrombin detection in the 6- and 10-bilayered GO film is estimated to be 0.1 and 0.001 nM, respectively, demonstrating the highly tunable nature of LbL-assembled GO multilayers in controlling the sensitivity of graphene-based FRET aptasensors.

In addition, the LbL-assembled graphene multilayer transistor can exhibit a photoresponsive property using pyrene-modified spiropyran molecule (Figure 4b).³¹ The spiropyran-functionalized graphene multilayer transistor exhibited the reversible switching of the Dirac point as well as changes in conductance induced by the photoswitchable property of the spiropyran group upon exposure to UV and visible light. Thus, the versatile nature of LbL assembly integrated with smart photoresponsive molecules as a means of controlling the device performance may be of potential interest in the design of new graphene-based optical electronic devices and sensors.

3.2.2. Tunable Characteristics of Graphene Multilayers. The chemical reduction and thermal annealing post treatments were utilized for the recovery of the electrical properties of the multilayered GO LbL films, resulting in their transformation into rGO multilayers. In rGO LbL films, both the sheet resistance and the transmittance can be effectively controlled by tuning the number of bilayers (Figure 5a).⁵ For example, the sheet resistance decreased linearly with an increasing number of bilayers in the region above four bilayers, whereas for two bilayers, an exceptionally high sheet resistance was observed due to the imperfect connection of the rGO sheets. Conversely, the transmittance measured at 550 nm decreased gradually with an increasing number of bilayers. Through LbL assembly, the sheet resistance and transmittance can be finely tuned in conjunction with the number of bilayers, which is strongly related to the thickness of the multilayers.

Utilizing the controllable characteristic of the electrical property by adjusting the number of rGO bilayers, the semiconducting characteristic in FET devices can also be elaborately regulated (Figure 5b).²³ Surprisingly, the fine variation in the number of bilayers resulted in a dramatic transition in the charge transport from p-type unipolar to ambipolar and eventually to n-type unipolar. These results indicate that more nitrogen doping occurs as the number of bilayers increases. The stacked and confined geometry of the LbL-assembled multilayer films possibly prevents facile escape of the nitrogen species. Therefore, the number of bilayers is the key factor in modulating both the nitrogen-doping level and thus electrical conductance of graphene multilayers. These interesting features highlight the advantages of LbL assembly as a nanoscale bottom-up assembly technique that is otherwise difficult to achieve using other methods.

3.3. Graphene Multilayers on Three-Dimensional (3D) Template. The LbL approach has the versatility to permit assembly on various substrates, particularly on 3D colloidal particles such as polymer beads, metal particles, and biomolecules.^{37,38,46,47} The removal of the colloid templates following the LbL multilayer deposition can result in hollow capsules.

Figure 6a shows the formation of graphene-based capsules through LbL assembly of surface functionalized rGO sheets of opposite charges onto polystyrene (PS) colloidal particles to

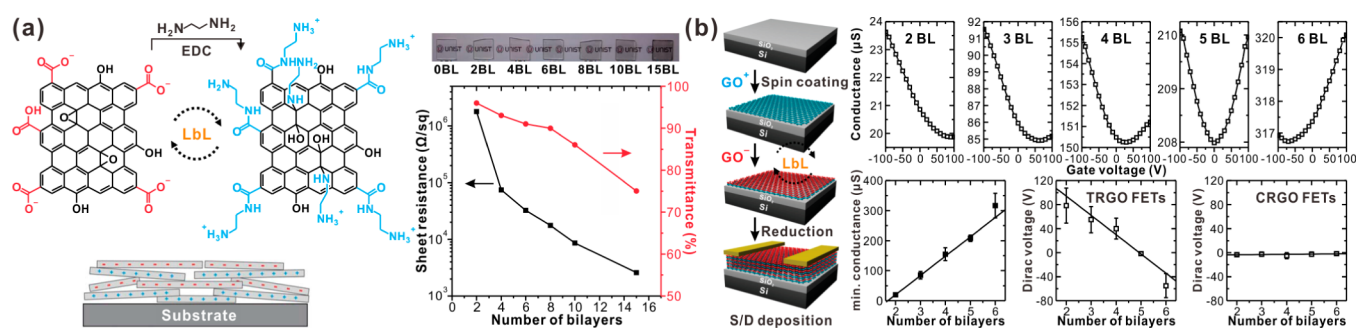


Figure 5. (a) Sheet resistance and transmittance of rGO multilayers from 2 to 15 bilayers after annealing in H_2/Ar atmosphere at $1000^\circ C$. Reprinted with permission from ref 5. Copyright 2011 Royal Society of Chemistry. (b) Transfer characteristics of thermally reduced GO FETs with various numbers of graphene bilayers. Reprinted with permission from ref 23. Copyright 2012 American Chemical Society.

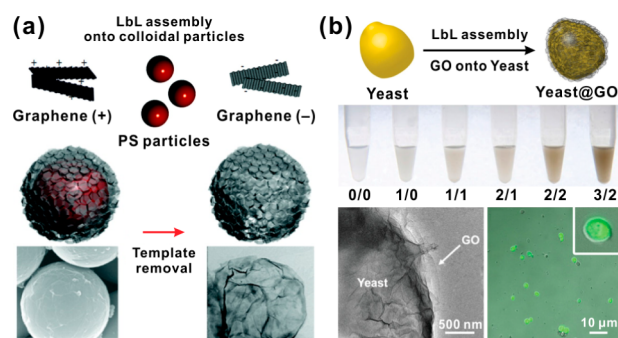


Figure 6. (a) Schematic illustration of the LbL assembly of rGO sheets onto PS colloidal particles and the hollow capsules with removal of the sacrificial template. Reprinted with permission from ref 38. Copyright 2010 American Chemical Society. (b) Encapsulation of yeast cell within GO sheets via LbL assembly. Reprinted with permission from ref 37. Copyright 2012 John Wiley and Sons.

produce multilayer thin films of graphene.³⁸ The subsequent removal of the sacrificial PS colloidal templates by THF treatment further resulted in the successful production of the hollow spherical graphene capsules. Following the successful graphene LbL assembly on a 3D spherical substrate as a model, living yeast cells were also encapsulated with GO multilayers to

construct a functional coating shell (Figure 6b).³⁷ The GO sheets with opposite charges were alternatively coated onto the individual yeast cells (yeast@GO). The coated GO shell demonstrated that the viability of the yeast cells was effectively preserved. In addition, yeast@GO preserved the original round shape of yeast, whereas the native yeast became highly shrunk due to dehydration during the sample preparation. Therefore, the LbL-assembled GO shell can afford an alternative bio-interfacing material with high biocompatibility to living cells.

This approach not only will provide a basis for designing hollow graphene capsules to create new possibilities in drug delivery, catalysts, and electrochemistry but can also be expanded to hybridizing the entries with GO sheets by integrating other organic polymers or inorganic nanoparticles through LbL self-assembly.

4. GRAPHENE/POLYMER ASSEMBLY

Polymeric materials have been widely used in LbL assembly due to their functional groups for electrostatic interactions or hydrogen bonding.^{64–67} In general, as-prepared GO is negatively charged in aqueous solution because of its functional groups, such as carboxylic acid and phenolic hydroxyl groups. Thus, positively charged polyelectrolytes have been selected for the counter component in graphene–polymer LbL assembly.^{19,56–58,60,62} In addition to the conventional electrostatic

Table 2. Summary of Graphene/Polymer Hybrids Based on LbL Assembly

material combination		substrate	system ($n = \text{no. of layers}$)	applications	ref
(+) component	(-) component				
PANI	GO	ITO/glass	$(PANI/GO)_n$	supercapacitor	48
PANI	GO	quartz	$(PANI/GO)_n$	electrode	49
PANI ^a	rGO	stainless steel	$(PANI/rGO)_n$	supercapacitor	50
PANI	PSS-GO	ITO/glass	$(PANI/PSS-GO)_n$	sensor	51
PDDA	GO	ITO/glass	$(PDDA/rGO)_n$	electrode	52
PDDA	GO	GCE	$(PDDA/rGO)_n$	electrocatalyst	53
PDDA	GO	Nafion	$(PDDA/GO)_n$	membrane	54
PEI	PAA-rGO	GCE	$(PEI/PAA-rGO)_n$	biosensing	55
PEI	GO	PET	$(PEI/GO)_n$	gas barrier	56
PEI	GO	PET	$(PEI/GO)_n$	gas barrier	57
PVA ^b	GO	quartz	$(PVA/GO/PVA/LDH)_n$	/	58
PVA ^b	GO	Si wafer	$(PVA/GO)_n$	/	59
PAH	GO	CaCO ₃	$(PAH/GO)_n$	drug encapsulation	60
poly-L-lysine	heparin-rGO	PCL scaffold	$(\text{poly-L-lysine/heparin-GO})_n$	neural scaffolds	61
QP4VP-co-PCN	rGO	ITO/glass	$(QP4VP-co-PCN/rGO)_n$	supercapacitor	62
chitosan-rGO-enzyme	PSS	Au/quartz	$(\text{Chitosan-rGO-enzyme/PSS})_n$	biosensing	63

^aElectro-polymerization during LbL process. ^bHydrogen bonding.

interaction in LbL assembly, hydrogen bonding can act as an attractive force between GO and the polymer due to abundant oxygen-functional groups in GO.^{20,59} Weak van der Waals interactions can also work in LbL assembly between GO and biopolymer and maximize its interactions along with other strong interactions, leading to the ultrarobust mechanical properties.^{68,69} The reduction of GO sheets in LbL film has been performed by thermal treatment, chemical reduction, and electrochemical reaction to restore the unique properties of graphene, while keeping the structure of polymer counterparts intact. Due to the outstanding mechanical properties of graphene, graphene-polymer nanocomposites have been widely studied for high performance materials by using graphene derivatives as nanofillers. For the mechanical properties of the graphene-polymer assembly, readers are encouraged to refer to the recent review for graphene-polymer nanocomposites by the Tsukruk group.¹⁵ In this section, we address recent progress in LbL assembly between graphene and polymeric materials based on the frequently used polymers, as summarized in Table 2.

4.1. Polyaniline (PANI). PANI is one of the most intensively investigated conducting polymers and has been considered a promising material for energy storage and conversion due to its excellent pseudocapacitive behavior, environmental stability, high electrical conductivity, low cost, and ease of synthesis.^{70–72} Because of these benefits, numerous techniques have been reported for synthesizing graphene/PANI nanocomposites.^{73–75} In particular, the emeraldine base form of PANI in acidic condition is appropriate to form a complex with GO sheets in the solution phase due to the electrostatic interactions.

Recently, our group reported a graphene/PANI hybrid electrode for supercapacitors using the LbL method based on the electrostatic interactions between the positively charged emeraldine base form of PANI and the negatively charged GO sheets (Figure 7).⁴⁸ The hybrid electrodes were assembled with the stable suspensions of PANI and GO in acidic conditions and were annealed and additionally reduced with hydrazine

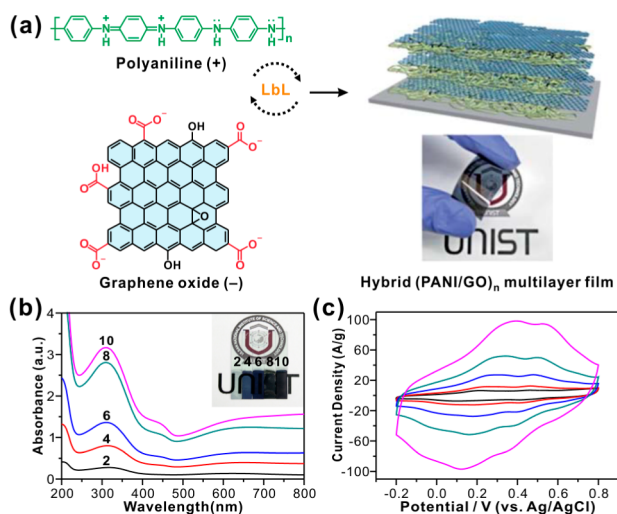


Figure 7. (a) Schematic illustration of LbL assembled (PANI/GO) multilayer thin film and (b) UV/vis spectra of as-assembled multilayer films as a function of the number of bilayers. (c) Cyclic voltammogram of heat-treated (PANI/GO)₁₀ film with various scan rates from 10 to 200 mV/s. Reprinted with permission from ref 48. Copyright 2012 Royal Society of Chemistry.

vapor to enhance the mechanical stability and electrical conductivity. The gravimetric capacitance was 375.2 F/g at a 0.5 A/g discharge current density. This LbL technique provides enhanced chemical stability and electronic conductivity during the charge-discharge process as well as precise control over the thickness and internal structure of the graphene/PANI hybrid supercapacitors. Similarly, Gao et al. suggested a sequential dip-coating of graphene sheets and electro-polymerization of aniline monomer to prepare the graphene/PANI hybrid supercapacitors.⁵⁰ In this case, the LbL structure of graphene/PANI was assembled by electrostatic interaction between negatively charged rGO and positively charged aniline monomer ions during the electro-polymerization. After the polymerization onto graphene sheets, the interfacial structure between graphene and PANI would be maintained with a van der Waals interaction for π - π stacking and hydrogen bonding interaction between functional groups. Due to the π - π stacking and the doping effect of the carboxyl and phenolic hydroxyl group of rGO in the LbL structure, the internal resistance of the graphene/PANI decreased compared with that of PANI.

The precise stacking of PANI and graphene sheets by the LbL method also makes it possible to improve the electrical conductivity, mechanical stability, and flexibility of the multilayered graphene/PANI thin films for electrochromic devices and electrochemical sensors based on the color change of PANI in different oxidation states. Shi et al. demonstrated an electrochromic behavior of graphene/PANI multilayer films by combining LbL assembly and chemical reduction without supporting conductive transparent electrodes.⁴⁹ The transmittance, electrical conductivity, and thickness of the film were controlled by adjusting the deposition number. In addition, the electrochemical sensing properties of a graphene/PANI multilayer were reported by the Liu group.⁵¹ The graphene sheets were stabilized with poly(sodium 4-styrenesulfonate) (PSS), which could act as a dopant for PANI in redox reactions, and the LbL multilayer film exhibited considerable electrocatalytic activity for H₂O₂.

4.2. Poly(diallyldimethylammonium chloride) (PDDA).

Typically, PDDA is used as an interlinker for diverse materials to form a complex in LbL assembly.^{76–78} Because of its transparency in UV-vis spectra, PDDA is also a promising material as a building block for optical and electronic devices. Using positively charged PDDA and negatively charged GO as building blocks, the Grätzel group demonstrated that the LbL-assembled graphene/PDDA could be used as counter electrodes in dye-sensitized solar cells (DSC).⁵² The LbL assembled film was reduced by the electrochemical reaction after the deposition to convert the GO into graphene (Figure 8). The

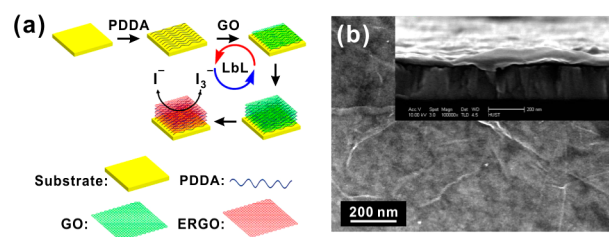


Figure 8. (a) Schematic representation of LbL assembly procedure for (graphene/PDDA)_n multilayer films and (b) FE-SEM image of (graphene/PDDA)₁₁/FTO with an inset of its cross-section. Reprinted with permission from ref 52. Copyright 2013 Nature Publishing Group.

electrocatalytic activities were enhanced by the electro-withdrawing ability of the positively charged PDDA compared with N-doped graphene films.⁷⁹ The DSC device using graphene/PDDA as a counter electrode exhibited power conversion efficiencies of 9.5% (with a low-volatility electrolyte system) and 7.6% (with a solvent-free ionic liquid electrolyte system). Using the same method, the LbL assembled graphene/PDDA films were also used in the metal-free electrocatalyst for the oxygen reduction reaction.⁵³

Yang et al. reported the surface modification of a Nafion membrane by the LbL deposition of PDDA and GO sheets to improve the methanol-blocking property of the pristine membrane in a passive direct methanol fuel cell.⁵⁴ The LbL-assembled Nafion membrane exhibited a decrease in the methanol diffusion coefficient by 67% compared with the pristine membrane, indicating that the graphene/PDDA multilayer is effective in suppressing the methanol permeability. Because the proton conductivity of the LbL-assembled membrane decreased upon increasing the number of bilayers, the membrane with two bilayers exhibited the best performance for the direct methanol fuel cell with a power density of 28.9 mW/cm², an increase of 60.6% with respect to the cell prepared with the pristine Nafion membrane.

4.3. Poly(ethylene imine) (PEI). In the LbL assembly technique, PEI has been widely used in surface modification to provide positively charged group on substrates due to its high positive charge density on the polymer backbone,^{55,61} however, here, we focus on the GO/PEI system as a graphene/polymer assembly.

The Grunlan group demonstrated that LbL-assembled GO/PEI on a PET film exhibited an extremely low oxygen permeability with improved H₂/CO₂ selectivity and high transparency.⁵⁶ A (GO/PEI)₁₀ film exhibited an oxygen permeability of 2.5 × 10⁻²⁰ cm² cm cm⁻² s⁻¹ Pa⁻¹, which would be comparable with a SiO_x nanocoating (Figure 9). In

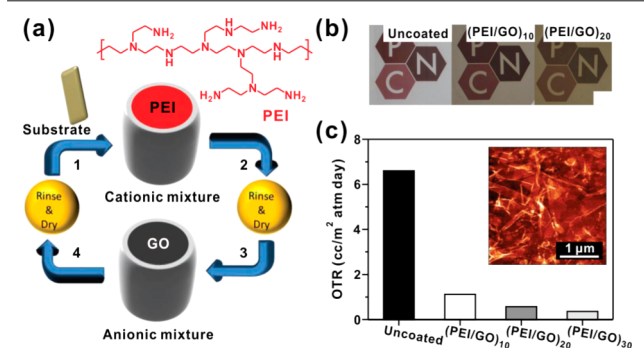


Figure 9. (a) Schematic illustration of LbL deposition process and (b) photographs of (GO/PEI)_n on PET film with the number of bilayer. (c) Oxygen transmission rate of (GO/PEI)_n films by 0.05 wt % GO suspensions. Inset indicates the AFM image of (GO/PEI)₁ on Si wafer using 0.05 wt % GO suspensions. Reprinted with permission from ref 56. Copyright 2013 John Wiley and Sons.

contrast with traditional polymer–polymer LbL assemblies, a graphene–polymer assembly provides a tightly packed nanobrick-wall-like structure with limited diffusion pathways for the gas molecules. Chen et al. also demonstrated a gas barrier film based on multilayered GO/PEI using similar methods.⁵⁷ The oxygen barrier properties of the GO/PEI film were significantly affected by the pH of the GO suspension as well as the number of bilayers. This result implies that the GO sheets and PEI are

tightly oriented and stacked with intercalated structures through the LbL method.

As a building block for graphene-based multilayer film, PEI was also successfully applied in LbL assembly by Zhang and co-workers.⁸⁰ To provide negatively charged functional groups on graphene, the graphene was stabilized with pyrene-grafted poly(acrylic acid). Additional PEI/glucoamylase LbL assembled layers were deposited onto the LbL film of graphene/PEI to construct a maltose sensing system, whose detection limit and sensitivity was 1.37 mM and 7.15 nA mM⁻¹ cm⁻², respectively.

4.4. Poly(vinyl alcohol) (PVA). The aforementioned interaction between graphene and the polymer in LbL assembly is almost based on electrostatic interactions. However, PVA possesses abundant hydroxyl groups (OH), which allows this polymer to form hydrogen bonding with oxygen functional groups on the surface of GO. Therefore, in this case, the hydrogen bonding could be the main driving force to achieve the graphene/PVA multilayer structure.

Zhao et al. demonstrated a significant enhancement in the mechanical properties of a GO/PVA film by LbL assembly.⁵⁹ Because of the well-defined layer structure arising from the hydrogen bonding and planar orientation of the GO layer in the PVA matrix, the elastic modulus and hardness of the hybrid film were increased by 98.7% and 240.4%, respectively, compared with the values for a pure PVA film. To investigate the difference between the LbL and vacuum-assisted filtration method, the Kotov group compared the two assembly methods for the rGO/PVA system.²⁰ The structural and thermal properties indicated that PVA in LbL composites could interact with a larger area of graphene and be more strongly constrained between graphene sheets than in filtrated composites, while the mechanical properties were almost identical for both methods at high graphene contents. In particular, the electrical conductivity of LbL composites was approximately ten times higher than that of the filtrated composites because the LbL composites were mainly affected by the tunneling barrier between graphene sheets. These differences imply that well-defined atomic and nanoscale organization in multilayer films by the LbL assembly would improve the specific properties correlated with structural orientation.

5. GRAPHENE/NANOPARTICLE ASSEMBLY

Even though many applicable nanoparticles exhibit superior electronic and catalytic properties as well as mechanically strong reinforcing effects, these nanoparticles often undergo a significant loss of intrinsic properties due to irreversible aggregation. Therefore, because graphene and nanoparticles can complement each other, graphene can be a favorable supporting material of nanoparticles. Furthermore, graphene/nanoparticle multilayered composites synthesized by the nanometer-scale control of LbL assembly exhibited improved performance compared with simply mixed hybrids. Using metal and oxide-based nanoparticles, many studies have been performed to apply LbL-assembled graphene/nanoparticle composites to diverse energy-related fields such as catalysts,^{81–84} supercapacitors,^{85–87} Li-ion batteries,⁸⁸ sensors,^{89–92} solar cells,^{93–96} and field-effect transistors,⁹⁷ which are summarized in Table 3. This graphene/nanoparticle assembly section will proceed in three parts: graphene/metal, graphene/metal oxide, and graphene/semiconductor.

5.1. Metal. LbL-assembled graphene/metal films could be implemented in electrochemical sensor technology such as for detecting H₂ and H₂O₂. For example, the Lange group

Table 3. Summary of Graphene/Nanoparticle Hybrids Based on LbL Assembly

material combination		substrate	system (n = no. of layers)	applications	ref
(+) component	(-) component				
Au NPs	GO	ITO	(Au/GO) $_n$	methanol oxidation	81
BSA-rGO	Au NPs	FTO	PEI/BSA-rGO/(BSA-rGO/Au NPs) $_n$	H ₂ O ₂ sensor	92
Au NPs ^a	GO	ITO	(GO/Au NPs) $_n$	supercapacitor	87
GO-IS-IL	Pt NPs	ITO	(GO-IS-IL/Pt NPs) $_n$	oxygen reduction	83
Pt NPs ^a	GO	CFE	(Pt NPs/GO) $_n$	methanol oxidation	84
Pd NPs	rGO	Au electrode	(rGO/Pd NPs) $_n$	H ₂ sensor	90
MWCNT	GO/TiO ₂ -Pd NPs	GCE	(NH ₂ -MWCNT/GT-Pd) $_n$	glucose sensor	89
PDDA	GO, PMA (MoO ₃)	Ti foil	(PDDA/GO/PDDA/PMA) $_n$	lithium ion battery	88
PDDA	PSS-rGO, MnO ₂ sheet	ITO	(PDDA/PSS-rGO/PDDA/MnO ₂) $_n$	supercapacitor	86
Co-Al LDH sheet	GO	ITO	PDDA/(Co-Al LDH/GO) $_n$	supercapacitor	85
PDDA	GO, TiO sheet	glass	(PDDA/GO/PDDA/TiO) $_n$	photoconductor	95
PEI	GO, Ti _{0.91} O ₂ sheet	ITO	(PEI/Ti _{0.91} O ₂ /PEI/GO) $_n$	photoconductor	93
CdSe	PAA-rGO	ITO	(PAA-rGO/CdSe) $_n$	aptasensor	91
rGO-PAH	CdS	FTO	(rGO-PAH/CdS) $_n$	photocatalyst	82
CdS ^b	GO, TiO ₂	FTO	(TNS/GO/CdS) $_n$	solar cell	96
CdS ^{a,b}	GO	ITO	(GO/CdS) $_n$	photoconductor	94
PAH	GO, H ₃ PW ₁₂ O ₄₀ ^c	Si wafer	(PAH/GO/PAH/PW) $_n$	FET	97

^aElectrodeposition. ^bSuccessive ionic layer adsorption and reaction (SILAR). ^cH₃PW₁₂O₄₀ (PW).

demonstrated that LbL-assembled graphene/palladium (Pd) nanoparticles films exhibit higher sensitivity to H₂ than graphene alone.⁹⁰ In addition, the Yang group reported that sensors for H₂O₂ detection with three-dimensional gold nanoparticle (Au NP) embedded porous graphene by LbL assembly exhibited further improved performance compared with non-porous graphene/AuNP composite films as well as 2D graphene/Au NP hybrid electrodes due to the higher surface area and improved permeability.⁹²

There are also examples of using an LbL-assembled graphene/metal electrode as an electrocatalyst. The Dong group fabricated LbL-assembled films with electrocatalytic activity toward oxygen reduction by alternatively assembling imidazolium-salt-based ionic liquid (IS-IL) functionalized graphene sheets and citrate-stabilized Pt nanoparticles (Pt NPs).⁸³ The introduction of IS-IL enhanced not only the conductivity of the as-prepared LbL films but also the dispersity of chemically modified graphene. 3D electrocatalytic thin films active toward methanol oxidation were also developed by integrating Au NPs with a GO support (Figure 10).⁸¹ The

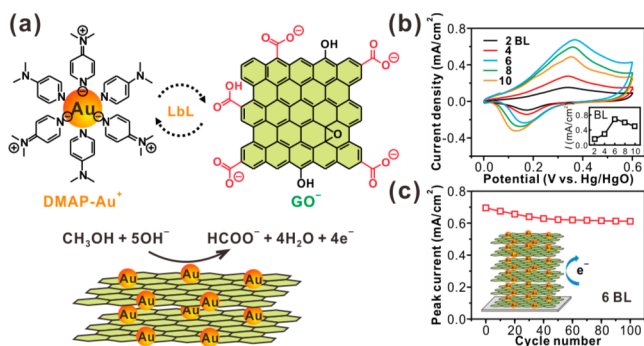


Figure 10. (a) Schematic representation of LbL assembled (Au NPs/GO) $_n$. (b) Cyclic voltamograms (CV) of (Au NPs/GO) $_n$ multilayer thin films and (c) cycling stability test of (Au NPs/GO) $_6$ after thermal treatment at 150 °C measured in 0.1 M KOH with 1.0 M CH₃OH. Reprinted with permission from ref 81. Copyright 2012 John Wiley and Sons.

results indicated that the current density of six-bilayer films is the highest due to the limited diffusion of methanol. It is also observed that Au NPs on graphene sheets exhibit an enhanced catalytic activity toward methanol oxidation after thermal reduction at 150 °C as post-treatment. Furthermore, the LbL method can not only control the amount of Au NPs on a graphene sheet but also enhance the stability of Au NPs when combined with a graphene sheet, emphasizing the critical role of graphene as a chemically stable support in preserving the catalytic active surface of Au NPs.

5.2. Metal Oxides. Although a metal oxide exhibits inferior electrical properties to the pure metal, its electroactivity can be supplemented by introducing graphene sheets. For example, the Yang group fabricated LbL-assembled poly(4-styrenesulfonic acid) (PSS)-mediated graphene sheet (PSS-rGO)/manganese dioxide (MnO₂) multilayered films for supercapacitors using PDDA as a linker.⁸⁶ Although MnO₂ has been limited for high-performance supercapacitors due to their poor electrical conductivity, this material exhibited a level of 90% of good cyclic stability after 1000 cycles and a capacitance of 263 F/g with a graphene-supported LbL structure.

The Huang group reported LbL-assembled thin films of MoO₂ nanoparticles and graphene sheets with three-dimensionally interconnected nanopores as binder-free anodes for lithium-ion batteries (Figure 11).⁸⁸ These researchers demonstrated that the electrochemical performance of a LbL-assembled MoO₂/graphene thin film is much better than that of a conventional anode composed of MoO₂ particulates. In addition, MoO₂ NPs were embedded in graphene with the 3D interconnected porosity of entire LbL films, which is favorable not only for access of the electrolyte to the surface of the anode but also for the sustainability of the volume change of active materials.

5.3. Semiconductors. Efficient electron collection and inhibition of electron-hole pair recombination are major issues in energy applications of semiconductor nanoparticles. Graphene acts as a good electron acceptor, generating electron transfers from a photoexcited semiconductor to graphene sheets. Some groups demonstrated that when titania nano-sheets are LbL assembled with graphene, the product can

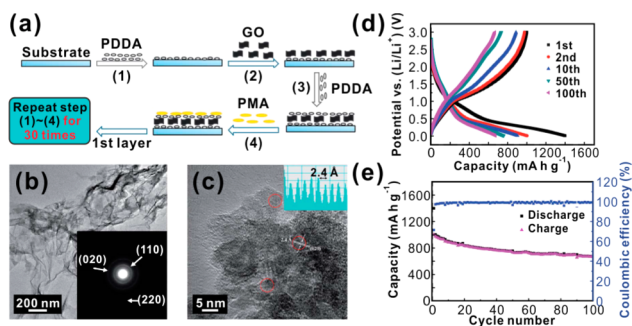


Figure 11. (a) Schematic representation, (b, c) TEM images of LbL assembled thin films with MoO₂ nanoparticles and graphene sheets, (d) galvanostatic discharge–charge curves, and (e) cycling stability and Coulombic efficiency of MoO₂ and graphene LbL films over 100 cycles at a current density of 0.01 mA/cm². Reprinted with permission from ref 88. Copyright 2012 Royal Society of Chemistry.

exhibit high photocurrent generation as well as ultrafast photocatalytic electron transfer with titania under UV irradiation.^{93,95} Taking advantage of these features, the Shi group fabricated two different nanoparticle-anchored glucose biosensors using negatively charged Pd NP-assembled graphene through UV reduction by TiO₂ (GTx-Pd), which was LbL assembled with positively charged MWCNTs-NH₂.⁸⁹

Quantum dots (QDs) can also act as photoassisted electron generators, utilizing light in the visible region due to size-dependent unique features. Recently, the Liu group constructed well-defined graphene/CdS QD multilayered films that exhibited improved photocatalytic reduction of substituted aromatic nitro compounds (Figure 12), where the positively

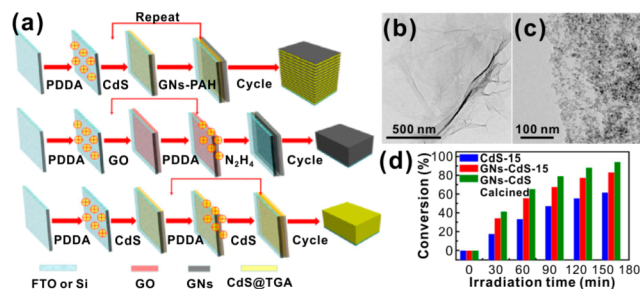


Figure 12. (a) Schematic representation of LbL assembled (rGO-PAH/CdS)_n, (PDDA/GO)_n, and (PDDA/CdS)_n films. TEM images of (b) PAH-modified graphene and (c) five bilayers of PAH-modified graphene/CdS QDs. (d) Photocatalytic reduction of 4-nitroaniline over (PDDA/CdS)₁₅, (rGO-PAH/CdS)₁₅, and calcined (rGO-PAH/CdS)₁₅ under visible light irradiation ($\lambda > 420$ nm). Reprinted with permission from ref 82. Copyright 2014 American Chemical Society.

charged poly(allylamine hydrochloride) (PAH) modified graphene and negatively charged CdS QDs were LbL self-assembled.⁸² These researchers demonstrated that the bandgap of CdS QDs in CdS/GO hybrid films becomes narrow with an increasing number of assembly cycles due to the interfacial contact between CdS QDs and graphene. As a result, these researchers proved that it is important to balance photon adsorption competition and interfacial interaction between CdS QDs and graphene sheets by changing the number of contacts between the CdS QDs and graphene. These controllable electroactivities on a three-dimensional LbL assembled electrocatalyst are a unique feature of the LbL architecture, which will be the subject of future studies.

6. SUMMARY AND OUTLOOK

The LbL assembly is a well-developed technique that makes it possible to assemble materials in diverse dimensions and has gradually expanded its application field owing to the simplicity of assembly principle and the consistency of quality. For the emerging nanomaterials with novel properties the LbL assembly has been chosen to design the hybrid nanostructures, and graphene is also no exception.

The recent advances in graphene-based nanocomposites by LbL assembly have been discussed in this review. This method allows the precise control of the charge transport behavior as well as of the general properties, such as the thickness, sheet resistance, and transmittance of the graphene hybrid films by simply adjusting the number of layers and assembly parameters. The introduction of graphene sheets by the LbL assembly can also enhance the intrinsic properties, such as the electrical conductivity, permeability, mechanical strength, and electrocatalytic activity, for the pristine polymeric materials. As a result, the LbL assembled graphene sheets play an important role in not only electron transport layer but also preventing aggregation of nanoparticles to maximize the electrical properties for the energy applications. Furthermore, several studies well demonstrated that the LbL assembled hybrid films are a promising candidate for shape-morphing^{98,99} or implantable devices^{100,101} by integrating the CNT based nanocomposite. Based on the remarkable performance of the carbon nanomaterials, we believe that the graphene-based nanocomposites will also provide new opportunities for the development of stimuli-responsive and wearable electronics.

Beyond the 2D assembled graphene materials, the graphene-based LbL assembly has been successfully applied to the 3D templates. This implies that the LbL assembly can offer a superb opportunity for designing various forms of graphene nanocomposites with desired properties required for advanced materials applications.

AUTHOR INFORMATION

Corresponding Author

*(B.-S.K.) E-mail: bskim19@unist.ac.kr.

Author Contributions

||T.L., S.H.M., M.G., and Y.K.J. contributed equally to this work.

Notes

The authors declare no competing financial interest.

ACKNOWLEDGMENTS

This work was supported by the National Research Foundation of Korea (NRF) Grants NRF-2014R1A2A1A11052829 and NRF-2015R1A1A3A04001437.

REFERENCES

- (1) Novoselov, K. S.; Geim, A. K.; Morozov, S. V.; Jiang, D.; Zhang, Y.; Dubonos, S. V.; Grigorieva, I. V.; Firsov, A. A. Electric Field Effect in Atomically Thin Carbon Films. *Science* **2004**, *306*, 666–669.
- (2) Stankovich, S.; Dikin, D. A.; Dommett, G. H. B.; Kohlhaas, K. M.; Zimney, E. J.; Stach, E. A.; Piner, R. D.; Nguyen, S. T.; Ruoff, R. S. Graphene-based Composite Materials. *Nature* **2006**, *442*, 282–286.
- (3) Geim, A. K.; Novoselov, K. S. The Rise of Graphene. *Nat. Mater.* **2007**, *6*, 183–191.
- (4) Hong, T.-K.; Lee, D. W.; Choi, H. J.; Shin, H. S.; Kim, B.-S. Transparent, Flexible Conducting Hybrid Multilayer Thin Films of Multiwalled Carbon Nanotubes with Graphene Nanosheets. *ACS Nano* **2010**, *4*, 3861–3868.

- (5) Lee, D. W.; Hong, T.-K.; Kang, D.; Lee, J.; Heo, M.; Kim, J. Y.; Kim, B.-S.; Shin, H. S. Highly Controllable Transparent and Conducting Thin Films Using Layer-by-Layer Assembly of Oppositely Charged Reduced Graphene Oxides. *J. Mater. Chem.* **2011**, *21*, 3438–3442.
- (6) Chen, P.; Xiao, T.-Y.; Qian, Y.-H.; Li, S.-S.; Yu, S.-H. A Nitrogen-Doped Graphene/Carbon Nanotube Nanocomposite with Synergistically Enhanced Electrochemical Activity. *Adv. Mater.* **2013**, *25*, 3192–3196.
- (7) Yu, D.; Yang, Y.; Durstock, M.; Baek, J.-B.; Dai, L. Soluble P3HT-Grafted Graphene for Efficient Bilayer–Heterojunction Photovoltaic Devices. *ACS Nano* **2010**, *4*, 5633–5640.
- (8) Kholmanov, I. N.; Domingues, S. H.; Chou, H.; Wang, X.; Tan, C.; Kim, J.-Y.; Li, H.; Piner, R.; Zharbin, A. J. G.; Ruoff, R. S. Reduced Graphene Oxide/Copper Nanowire Hybrid Films as High-Performance Transparent Electrodes. *ACS Nano* **2013**, *7*, 1811–1816.
- (9) Johnston, A. P. R.; Cortez, C.; Angelatos, A. S.; Caruso, F. Layer-by-Layer Engineered Capsules and Their Applications. *Curr. Opin. Colloid Interface Sci.* **2006**, *11*, 203–209.
- (10) Ariga, K.; Hill, J. P.; Ji, Q. Layer-by-Layer Assembly as a Versatile Bottom-up Nanofabrication Technique for Exploratory Research and Realistic Application. *Phys. Chem. Chem. Phys.* **2007**, *9*, 2319–2340.
- (11) Yang, M.; Hou, Y.; Kotov, N. A. Graphene-based Multilayers: Critical Evaluation of Materials Assembly Techniques. *Nano Today* **2012**, *7*, 430–447.
- (12) Ariga, K.; Yamauchi, Y.; Rydzek, G.; Ji, Q.; Yonamine, Y.; Wu, K. C. W.; Hill, J. P. Layer-by-Layer Nanoarchitectonics: Invention, Innovation, and Evolution. *Chem. Lett.* **2014**, *43*, 36–68.
- (13) Wang, Y.; Angelatos, A. S.; Caruso, F. Template Synthesis of Nanostructured Materials via Layer-by-Layer Assembly. *Chem. Mater.* **2007**, *20*, 848–858.
- (14) Yan, Y.; Björnmalin, M.; Caruso, F. Assembly of Layer-by-Layer Particles and Their Interactions with Biological Systems. *Chem. Mater.* **2013**, *26*, 452–460.
- (15) Hu, K.; Kulkarni, D. D.; Choi, I.; Tsukruk, V. V. Graphene-Polymer Nanocomposites for Structural and Functional Applications. *Prog. Polym. Sci.* **2014**, *39*, 1934–1972.
- (16) Iler, R. K. Multilayers of Colloidal Particles. *J. Colloid Interface Sci.* **1966**, *21*, 569–594.
- (17) Decher, G. Fuzzy Nanoassemblies: Toward Layered Polymeric Multicomposites. *Science* **1997**, *277*, 1232–1237.
- (18) Kotov, N. A.; Dékány, I.; Fendler, J. H. Ultrathin Graphite oxide–Polyelectrolyte Composites Prepared by Self-assembly: Transition between Conductive and Non-Conductive States. *Adv. Mater.* **1996**, *8*, 637–641.
- (19) Kovtyukhova, N. I.; Ollivier, P. J.; Martin, B. R.; Mallouk, T. E.; Chizhik, S. A.; Buzaneva, E. V.; Gorchinskiy, A. D. Layer-by-Layer Assembly of Ultrathin Composite Films from Micron-Sized Graphite Oxide Sheets and Polycations. *Chem. Mater.* **1999**, *11*, 771–778.
- (20) Zhu, J.; Zhang, H.; Kotov, N. A. Thermodynamic and Structural Insights into Nanocomposites Engineering by Comparing Two Materials Assembly Techniques for Graphene. *ACS Nano* **2013**, *7*, 4818–4829.
- (21) Ariga, K.; Yamauchi, Y.; Mori, T.; Hill, J. P. 25th Anniversary Article: What Can Be Done with the Langmuir-Blodgett Method? Recent Developments and its Critical Role in Materials Science. *Adv. Mater.* **2013**, *25*, 6477–6512.
- (22) Ma, R.; Sasaki, T. Nanosheets of Oxides and Hydroxides: Ultimate 2D Charge-Bearing Functional Crystallites. *Adv. Mater.* **2010**, *22*, 5082–5104.
- (23) Hwang, H.; Joo, P.; Kang, M. S.; Ahn, G.; Han, J. T.; Kim, B.-S.; Cho, J. H. Highly Tunable Charge Transport in Layer-by-Layer Assembled Graphene Transistors. *ACS Nano* **2012**, *6*, 2432–2440.
- (24) Cho, J.; Char, K.; Hong, J. D.; Lee, K. B. Fabrication of Highly Ordered Multilayer Films Using a Spin Self-Assembly Method. *Adv. Mater.* **2001**, *13*, 1076–1078.
- (25) Schlenoff, J. B.; Dubas, S. T.; Farhat, T. Sprayed Polyelectrolyte Multilayers. *Langmuir* **2000**, *16*, 9968–9969.
- (26) Krogman, K. C.; Lowery, J. L.; Zacharia, N. S.; Rutledge, G. C.; Hammond, P. T. Spraying Asymmetry into Functional Membranes Layer-by-Layer. *Nat. Mater.* **2009**, *8*, 512–518.
- (27) Lee, S. W.; Kim, B.-S.; Chen, S.; Shao-Horn, Y.; Hammond, P. T. Layer-by-Layer Assembly of All Carbon Nanotube Ultrathin Films for Electrochemical Applications. *J. Am. Chem. Soc.* **2008**, *131*, 671–679.
- (28) Kim, B.-S.; Lee, S. W.; Yoon, H.; Strano, M. S.; Shao-Horn, Y.; Hammond, P. T. Pattern Transfer Printing of Multiwalled Carbon Nanotube Multilayers and Application in Biosensors. *Chem. Mater.* **2010**, *22*, 4791–4797.
- (29) Lee, S. W.; Yabuuchi, N.; Gallant, B. M.; Chen, S.; Kim, B.-S.; Hammond, P. T.; Shao-Horn, Y. High-Power Lithium Batteries from Functionalized Carbon-Nanotube Electrodes. *Nat. Nanotechnol.* **2010**, *5*, 531–537.
- (30) Wang, X.; Wang, J.; Cheng, H.; Yu, P.; Ye, J.; Mao, L. Graphene as a Spacer to Layer-by-Layer Assemble Electrochemically Functionalized Nanostructures for Molecular Bioelectronic Devices. *Langmuir* **2011**, *27*, 11180–11186.
- (31) Joo, P.; Kim, B. J.; Jeon, E. K.; Cho, J. H.; Kim, B.-S. Optical Switching of The Dirac Point in Graphene Multilayer Field-Effect Transistors Functionalized with Spiropyran. *Chem. Commun.* **2012**, *48*, 10978–10980.
- (32) Jung, Y. K.; Lee, T.; Shin, E.; Kim, B.-S. Highly Tunable Aptasensing Microarrays with Graphene Oxide Multilayers. *Sci. Rep.* **2013**, *3*, 3367.
- (33) Sydlík, S. A.; Swager, T. M. Functional Graphenic Materials via a Johnson–Claisen Rearrangement. *Adv. Funct. Mater.* **2013**, *23*, 1873–1882.
- (34) Park, J. S.; Cho, S. M.; Kim, W.-J.; Park, J.; Yoo, P. J. Fabrication of Graphene Thin Films Based on Layer-by-Layer Self-Assembly of Functionalized Graphene Nanosheets. *ACS Appl. Mater. Interfaces* **2011**, *3*, 360–368.
- (35) Ou, X.; Jiang, L.; Chen, P.; Zhu, M.; Hu, W.; Liu, M.; Zhu, J.; Ju, H. Highly Stable Graphene-Based Multilayer Films Immobilized via Covalent Bonds and Their Applications in Organic Field-Effect Transistors. *Adv. Funct. Mater.* **2013**, *23*, 2422–2435.
- (36) Zhu, Y.; Tour, J. M. Graphene Nanoribbon Thin Films Using Layer-by-Layer Assembly. *Nano Lett.* **2010**, *10*, 4356–4362.
- (37) Yang, S. H.; Lee, T.; Seo, E.; Ko, E. H.; Choi, I. S.; Kim, B.-S. Interfacing Living Yeast Cells with Graphene Oxide Nanosheets. *Macromol. Biosci.* **2012**, *12*, 61–66.
- (38) Hong, J.; Char, K.; Kim, B.-S. Hollow Capsules of Reduced Graphene Oxide Nanosheets Assembled on a Sacrificial Colloidal Particle. *J. Phys. Chem. Lett.* **2010**, *1*, 3442–3445.
- (39) Unarunotai, S.; Koepke, J. C.; Tsai, C.-L.; Du, F.; Chialvo, C. E.; Murata, Y.; Haasch, R.; Petrov, I.; Mason, N.; Shim, M.; Lyding, J.; Rogers, J. A. Layer-by-Layer Transfer of Multiple, Large Area Sheets of Graphene Grown in Multilayer Stacks on a Single SiC Wafer. *ACS Nano* **2010**, *4*, 5591–5598.
- (40) Wang, Y.; Tong, S. W.; Xu, X. F.; Özyilmaz, B.; Loh, K. P. Interface Engineering of Layer-by-Layer Stacked Graphene Anodes for High-Performance Organic Solar Cells. *Adv. Mater.* **2011**, *23*, 1514–1518.
- (41) Kang, J.; Kim, H.; Kim, K. S.; Lee, S.-K.; Bae, S.; Ahn, J.-H.; Kim, Y.-J.; Choi, J.-B.; Hong, B. H. High-Performance Graphene-Based Transparent Flexible Heaters. *Nano Lett.* **2011**, *11*, 5154–5158.
- (42) Chen, J.-J.; Meng, J.; Zhou, Y.-B.; Wu, H.-C.; Bie, Y.-Q.; Liao, Z.-M.; Yu, D.-P. Layer-by-Layer Assembly of Vertically Conducting Graphene Devices. *Nat. Commun.* **2013**, *4*, 1921.
- (43) Liang, Q.; Yao, X.; Wang, W.; Liu, Y.; Wong, C. P. A Three-Dimensional Vertically Aligned Functionalized Multilayer Graphene Architecture: An Approach for Graphene-Based Thermal Interfacial Materials. *ACS Nano* **2011**, *5*, 2392–2401.
- (44) Xie, X.; Qu, L.; Zhou, C.; Li, Y.; Zhu, J.; Bai, H.; Shi, G.; Dai, L. An Asymmetrically Surface-Modified Graphene Film Electrochemical Actuator. *ACS Nano* **2010**, *4*, 6050–6054.
- (45) Zheng, Q.; Ip, W. H.; Lin, X.; Yousefi, N.; Yeung, K. K.; Li, Z.; Kim, J.-K. Transparent Conductive Films Consisting of Ultralarge

Graphene Sheets Produced by Langmuir–Blodgett Assembly. *ACS Nano* **2011**, *5*, 6039–6051.

(46) Yoon, S.-M.; Choi, W. M.; Baik, H.; Shin, H.-J.; Song, I.; Kwon, M.-S.; Bae, J. J.; Kim, H.; Lee, Y. H.; Choi, J.-Y. Synthesis of Multilayer Graphene Balls by Carbon Segregation from Nickel Nanoparticles. *ACS Nano* **2012**, *6*, 6803–6811.

(47) Chen, Q.; Zhang, C.; Xue, F.; Zhou, Y.; Li, W.; Wang, Y.; Tu, W.; Zou, Z.; Wang, X.; Xiao, M. Enhanced Hot-Carrier Luminescence in Multilayer Reduced Graphene Oxide Nanospheres. *Sci. Rep.* **2013**, *3*, 2315.

(48) Lee, T.; Yun, T.; Park, B.; Sharma, B.; Song, H. K.; Kim, B. S. Hybrid Multilayer Thin Film Supercapacitor of Graphene Nanosheets with Polyaniline: Importance of Establishing Intimate Electronic Contact through Nanoscale Blending. *J. Mater. Chem.* **2012**, *22*, 21092–21099.

(49) Sheng, K.; Bai, H.; Sun, Y.; Li, C.; Shi, G. Layer-by-Layer Assembly of Graphene/Polyaniline Multilayer Films and Their Application for Electrochromic Devices. *Polymer* **2011**, *52*, 5567–5572.

(50) Gao, Z.; Yang, W.; Wang, J.; Yan, H.; Yao, Y.; Ma, J.; Wang, B.; Zhang, M.; Liu, L. Electrochemical Synthesis of Layer-by-Layer Reduced Graphene Oxide Sheets/Polyaniline Nanofibers Composite and Its Electrochemical Performance. *Electrochim. Acta* **2013**, *91*, 185–194.

(51) Luo, J.; Chen, Y.; Ma, Q.; Liu, R.; Liu, X. Layer-by-Layer Self-Assembled Hybrid Multilayer Films Based on Poly(sodium 4-styrenesulfonate) Stabilized Graphene with Polyaniline and Their Electrochemical Sensing Properties. *RSC Adv.* **2013**, *3*, 17866–17873.

(52) Xu, X.; Huang, D.; Cao, K.; Wang, M.; Zakeeruddin, S. M.; Grätzel, M. Electrochemically Reduced Graphene Oxide Multilayer Films as Efficient Counter Electrode for Dye-Sensitized Solar Cells. *Sci. Rep.* **2013**, *3*, 1489.

(53) Huang, D.; Zhang, B.; Zhang, Y.; Zhan, F.; Xu, X.; Shen, Y.; Wang, M. Electrochemically Reduced Graphene Oxide Multilayer Films as Metal-Free Electrocatalysts for Oxygen Reduction. *J. Mater. Chem. A* **2013**, *1*, 1415–1420.

(54) Yuan, T.; Pu, L.; Huang, Q.; Zhang, H.; Li, X.; Yang, H. An Effective Methanol-Blocking Membrane Modified with Graphene Oxide Nanosheets for Passive Direct Methanol Fuel Cells. *Electrochim. Acta* **2014**, *117*, 393–397.

(55) Pei, R.; Cui, X.; Yang, X.; Wang, E. Assembly of Alternating Polycation and DNA Multilayer Films by Electrostatic Layer-by-Layer Adsorption. *Biomacromolecules* **2001**, *2*, 463–468.

(56) Yang, Y. H.; Bolling, L.; Priolo, M. A.; Grunlan, J. C. Super gas barrier and selectivity of graphene oxide-polymer multilayer thin films. *Adv. Mater.* **2013**, *25*, 503–508.

(57) Chen, J. T.; Fu, Y. J.; An, Q. F.; Lo, S. C.; Huang, S. H.; Hung, W. S.; Hu, C. C.; Lee, K. R.; Lai, J. Y. Tuning Nanostructure of Graphene Oxide/Polyelectrolyte LbL Assemblies by Controlling pH of GO Suspension to Fabricate Transparent and Super Gas Barrier Films. *Nanoscale* **2013**, *5*, 9081–9088.

(58) Chen, D.; Wang, X.; Liu, T.; Wang, X.; Li, J. Electrically Conductive Poly(vinyl alcohol) Hybrid Films Containing Graphene and Layered Double Hydroxide Fabricated via Layer-by-Layer Self-Assembly. *ACS Appl. Mater. Interfaces* **2010**, *2*, 2005–2011.

(59) Zhao, X.; Zhang, Q.; Hao, Y.; Li, Y.; Fang, Y.; Chen, D. Alternate Multilayer Films of Poly(vinyl alcohol) and Exfoliated Graphene Oxide Fabricated via A Facial Layer-by-Layer Assembly. *Macromolecules* **2010**, *43*, 9411–9416.

(60) Kurapati, R.; Raichur, A. M. Graphene Oxide Based Multilayer Capsules with Unique Permeability Properties: Facile Encapsulation of Multiple Drugs. *Chem. Commun.* **2012**, *48*, 6013–6015.

(61) Zhou, K.; Thouas, G. A.; Bernard, C. C.; Nisbet, D. R.; Finkelstein, D. I.; Li, D.; Forsythe, J. S. Method to Impart Electro- and Biofunctionality to Neural Scaffolds Using Graphene-Polyelectrolyte Multilayers. *ACS Appl. Mater. Interfaces* **2012**, *4*, 4524–4531.

(62) Wang, D.; Wang, X. Self-Assembled Graphene/Azo Polyelectrolyte Multilayer Film and Its Application in Electrochemical Energy Storage Device. *Langmuir* **2011**, *27*, 2007–2013.

(63) Barsan, M. M.; David, M.; Florescu, M.; Țugulea, L.; Brett, C. M. A. A New Self-Assembled Layer-by-Layer Glucose Biosensor Based on Chitosan Biopolymer Entrapped Enzyme with Nitrogen Doped Graphene. *Bioelectrochemistry* **2014**, *99*, 46–52.

(64) Shiratori, S. S.; Rubner, M. F. pH-Dependent Thickness Behavior of Sequentially Adsorbed Layers of Weak Polyelectrolytes. *Macromolecules* **2000**, *33*, 4213–4219.

(65) Chen, W.; McCarthy, T. J. Layer-by-Layer Deposition: A Tool for Polymer Surface Modification. *Macromolecules* **1997**, *30*, 78–86.

(66) Nguyen, C. A.; Argun, A. A.; Hammond, P. T.; Lu, X.; Lee, P. S. Layer-by-Layer Assembled Solid Polymer Electrolyte for Electrochromic Devices. *Chem. Mater.* **2011**, *23*, 2142–2149.

(67) Kharlampieva, E.; Koziyovskaya, V.; Sukhishvili, S. A. Layer-by-Layer Hydrogen-Bonded Polymer Films: From Fundamentals to Applications. *Adv. Mater.* **2009**, *21*, 3053–3065.

(68) Hu, K.; Gupta, M. K.; Kulkarni, D. D.; Tsukruk, V. V. Ultra-Robust Graphene Oxide-Silk Fibroin Nanocomposite Membranes. *Adv. Mater.* **2013**, *25*, 2301–2307.

(69) Hu, K.; Tolentino, L. S.; Kulkarni, D. D.; Ye, C.; Kumar, S.; Tsukruk, V. V. Written-in Conductive Patterns on Robust Graphene Oxide Biopaper by Electrochemical Microstamping. *Angew. Chem., Int. Ed.* **2013**, *52*, 13784–13788.

(70) Meng, C.; Liu, C.; Chen, L.; Hu, C.; Fan, S. Highly Flexible and All-Solid-State Paperlike Polymer Supercapacitors. *Nano Lett.* **2010**, *10*, 4025–4031.

(71) Hyder, M. N.; Lee, S. W.; Cebeci, F. C.; Schmidt, D. J.; Shao-Horn, Y.; Hammond, P. T. Layer-by-Layer Assembled Polyaniline Nanofiber/Multiwall Carbon Nanotube Thin Film Electrodes for High-Power and High-Energy Storage Applications. *ACS Nano* **2011**, *5*, 8552–8561.

(72) Wang, K.; Huang, J.; Wei, Z. Conducting Polyaniline Nanowire Arrays for High Performance Supercapacitors. *J. Phys. Chem. C* **2010**, *114*, 8062–8067.

(73) Zhang, K.; Zhang, L. L.; Zhao, X. S.; Wu, J. Graphene/Polyaniline Nanofiber Composites as Supercapacitor Electrodes. *Chem. Mater.* **2010**, *22*, 1392–1401.

(74) Xu, J.; Wang, K.; Zu, S. Z.; Han, B. H.; Wei, Z. Hierarchical Nanocomposites of Polyaniline Nanowire Arrays on Graphene Oxide Sheets with Synergistic Effect for Energy Storage. *ACS Nano* **2010**, *4*, 5019–5026.

(75) Kim, M.; Lee, C.; Jang, J. Fabrication of Highly Flexible, Scalable, and High-Performance Supercapacitors Using Polyaniline/Reduced Graphene Oxide Film with Enhanced Electrical Conductivity and Crystallinity. *Adv. Funct. Mater.* **2014**, *24*, 2489–2499.

(76) Zhang, L.; Chen, H.; Sun, J.; Shen, J. Layer-by-Layer Deposition of Poly(diallyldimethylammonium chloride) and Sodium Silicate Multilayers on Silica-Sphere-Coated Substrate-Facile Method to Prepare A Superhydrophobic Surface. *Chem. Mater.* **2007**, *19*, 948–953.

(77) Jiao, Q.; Yi, Z.; Chen, Y.; Xi, F. Dendronized Polymer as Building Block for Layer-by-Layer Assembly: Polyelectrolyte Multilayer Films for Incorporation and Controlled Release of Water-Insoluble Dye. *Polymer* **2008**, *49*, 1520–1526.

(78) Park, Y. T.; Ham, A. Y.; Yang, Y. H.; Grunlan, J. C. Fully Organic ITO Replacement Through Acid Doping of Double-Walled Carbon Nanotube Thin Film Assemblies. *RSC Adv.* **2011**, *1*, 662–671.

(79) Yen, M. Y.; Hsieh, C. K.; Teng, C. C.; Hsiao, M. C.; Liu, P. I.; Ma, C. C. M.; Tsai, M. C.; Tsai, C. H.; Lin, Y. R.; Chou, T. Y. Metal-Free, Nitrogen-Doped Graphene Used as A Novel Catalyst for Dye-Sensitized Solar Cell Counter Electrodes. *RSC Adv.* **2012**, *2*, 2725–2728.

(80) Zeng, G.; Xing, Y.; Gao, J.; Wang, Z.; Zhang, X. Unconventional Layer-by-Layer Assembly of Graphene Multilayer Films for Enzyme-Based Glucose and Maltose Biosensing. *Langmuir* **2010**, *26*, 15022–15026.

(81) Choi, Y.; Gu, M.; Park, J.; Song, H.-K.; Kim, B.-S. Graphene Multilayer Supported Gold Nanoparticles for Efficient Electrocatalysts Toward Methanol Oxidation. *Adv. Energy Mater.* **2012**, *2*, 1510–1518.

(82) Xiao, F.-X.; Miao, J.; Liu, B. Layer-by-Layer Self-Assembly of CdS Quantum Dots/Graphene Nanosheets Hybrid Films for Photoelectrochemical and Photocatalytic Applications. *J. Am. Chem. Soc.* **2014**, *136*, 1559–1569.

(83) Zhu, C.; Guo, S.; Zhai, Y.; Dong, S. Layer-by-Layer Self-Assembly for Constructing a Graphene/Platinum Nanoparticle Three-Dimensional Hybrid Nanostructure Using Ionic Liquid as a Linker. *Langmuir* **2010**, *26*, 7614–7618.

(84) Yao, Z.; Yue, R.; Zhai, C.; Jiang, F.; Wang, H.; Du, Y.; Wang, C.; Yang, P. Electrochemical Layer-by-Layer Fabrication of A Novel Three-Dimensional Pt/Graphene/Carbon Fiber Electrode and Its Improved Catalytic Performance for Methanol Electrooxidation in Alkaline Medium. *Int. J. Hydrogen Energy* **2013**, *38*, 6368–6376.

(85) Dong, X.; Wang, L.; Wang, D.; Li, C.; Jin, J. Layer-by-Layer Engineered Co-Al Hydroxide Nanosheets/Graphene Multilayer Films as Flexible Electrode for Supercapacitor. *Langmuir* **2012**, *28*, 293–298.

(86) Li, Z.; Wang, J.; Liu, X.; Liu, S.; Ou, J.; Yang, S. Electrostatic Layer-by-Layer Self-Assembly Multilayer Films Based on Graphene and Manganese Dioxide Sheets as Novel Electrode Materials for Supercapacitors. *J. Mater. Chem.* **2011**, *21*, 3397–3403.

(87) Niu, Z.; Du, J.; Cao, X.; Sun, Y.; Zhou, W.; Hng, H. H.; Ma, J.; Chen, X.; Xie, S. Electrophoretic Build-Up of Alternately Multilayered Films and Micropatterns Based on Graphene Sheets and Nanoparticles and their Applications in Flexible Supercapacitors. *Small* **2012**, *8*, 3201–3208.

(88) Xia, F.; Hu, X.; Sun, Y.; Luo, W.; Huang, Y. Layer-by-Layer Assembled MoO₂-Graphene Thin Film as A High-Capacity and Binder-Free Anode for Lithium-Ion Batteries. *Nanoscale* **2012**, *4*, 4707–4711.

(89) Yu, Y.; Yang, Y.; Gu, H.; Yu, D.; Shi, G. Size-Controllable Preparation of Palladium Nanoparticles Assembled on TiO₂/Graphene Nanosheets and Their Electrocatalytic Activity for Glucose Biosensing. *Anal. Methods* **2013**, *5*, 7049–7057.

(90) Lange, U.; Hirsch, T.; Mirsky, V. M.; Wolfbeis, O. S. Hydrogen Sensor Based on A Graphene - Palladium Nanocomposite. *Electrochim. Acta* **2011**, *56*, 3707–3712.

(91) Zhang, X.; Li, S.; Jin, X.; Zhang, S. A New Photoelectrochemical Aptasensor for The Detection of Thrombin Based on Functionalized Graphene and CdSe Nanoparticles Multilayers. *Chem. Commun.* **2011**, *47*, 4929–4931.

(92) Xi, Q.; Chen, X.; Evans, D. G.; Yang, W. Gold Nanoparticle-Embedded Porous Graphene Thin Films Fabricated via Layer-by-Layer Self-Assembly and Subsequent Thermal Annealing for Electrochemical Sensing. *Langmuir* **2012**, *28*, 9885–9892.

(93) Manga, K. K.; Zhou, Y.; Yan, Y.; Loh, K. P. Multilayer Hybrid Films Consisting of Alternating Graphene and Titania Nanosheets with Ultrafast Electron Transfer and Photoconversion Properties. *Adv. Funct. Mater.* **2009**, *19*, 3638–3643.

(94) Guo, C. X.; Yang, H. B.; Sheng, Z. M.; Lu, Z. S.; Song, Q. L.; Li, C. M. Layered Graphene/Quantum Dots for Photovoltaic Devices. *Angew. Chem., Int. Ed.* **2010**, *49*, 3014–3017.

(95) Yao, H.-B.; Wu, L.-H.; Cui, C.-H.; Fang, H.-Y.; Yu, S.-H. Direct Fabrication of Photoconductive Patterns on LBL Assembled Graphene Oxide/PDDA/Titania Hybrid Films by Photothermal and Photocatalytic Reduction. *J. Mater. Chem.* **2010**, *20*, 5190–5195.

(96) Wang, K.; Wan, S.; Liu, Q.; Yang, N.; Zhai, J. CdS Quantum Dot-Decorated Titania/Graphene Nanosheets Stacking Structures for Enhanced Photoelectrochemical Solar Cells. *RSC Adv.* **2013**, *3*, 23755–23761.

(97) Li, H.; Pang, S.; Wu, S.; Feng, X.; Müllen, K.; Bubeck, C. Layer-by-Layer Assembly and UV Photoreduction of Graphene–Polyoxometalate Composite Films for Electronics. *J. Am. Chem. Soc.* **2011**, *133*, 9423–9429.

(98) Andres, C. M.; Zhu, J.; Shyu, T.; Flynn, C.; Kotov, N. A. Shape-Morphing Nanocomposite Origami. *Langmuir* **2014**, *30*, 5378–5385.

(99) Shenoy, V. B.; Gracias, D. H. Self-Folding Thin-Film Materials: From Nanopolyhedra to Graphene Origami. *MRS Bull.* **2012**, *37*, 847–854.

(100) Zhang, H.; Patel, P. R.; Xie, Z.; Swanson, S. D.; Wang, X.; Kotov, N. A. Tissue-Compliant Neural Implants from Microfabricated Carbon Nanotube Multilayer Composite. *ACS Nano* **2013**, *7*, 7619–7629.

(101) Kozai, T. D. Y.; Langhals, N. B.; Patel, P. R.; Deng, X.; Zhang, H.; Smith, K. L.; Lahann, J.; Kotov, N. A.; Kipke, D. R. Ultrasmall Implantable Composite Microelectrodes with Bioactive Surfaces for Chronic Neural Interfaces. *Nat. Mater.* **2012**, *11*, 1065–1073.

■ NOTE ADDED AFTER ASAP PUBLICATION

There were errors in Tables 2 and 3 in the version published ASAP on May 14, 2015; the corrected version was published ASAP on May 20, 2015.